

Received September 19, 2020, accepted September 28, 2020, date of publication October 1, 2020, date of current version October 13, 2020.

Digital Object Identifier 10.1109/ACCESS.2020.3028081

Fractional-Order New Generation of $nk \pm m$ -Order Harmonic Repetitive Control for PWM Converters

WEI WANG¹, WENZHOU LU¹, (Member, IEEE), KELIANG ZHOU², (Senior Member, IEEE), AND QIGAO FAN¹, (Member, IEEE)

¹Key Laboratory of Advanced Process Control for Light Industry, School of Internet of Things Engineering, Ministry of Education, Jiangnan University, Wuxi 214122, China

²School of Automation, Wuhan University of Technology, Wuhan 430070, China

Corresponding author: Wenzhou Lu (luwenzhou@126.com)


This work was supported in part by the National Natural Science Foundation of China under Grant 51407084 and Grant 61673305, in part by the China Postdoctoral Science Foundation under Grant 2017M610294, in part by the Jiangsu Planned Projects for Postdoctoral Research Funds under Grant 1701092B, and in part by the “Postgraduate Research and Practice Innovation Program of Jiangnan University” under Grant JNKY19_060.

ABSTRACT In this paper, a fractional-order new generation of $nk \pm m$ -order harmonic repetitive controller (FO-NG- $nk \pm m$ RC), composed of a proposed new generation of $nk \pm m$ RC (NG- $nk \pm m$ RC) and a Taylor Series expansion based fractional delay (FD) filter using Lagrange interpolation with Farrow structure, is proposed. Compared with conventional $nk \pm m$ RC, NG- $nk \pm m$ RC has more advantages while achieving the same performance as the conventional $nk \pm m$ RC. Different FD approximation algorithms are compared for the first time from the perspective of controller computational burden. The inner relationship between Taylor Series expansion method and Farrow structure FD filter is explained, detailed mathematical derivation is provided, and a complete set of FD filter design methods is formed. When the fundamental frequency is not constant, the performance of $nk \pm m$ RC to track or eliminate any specific $nk \pm m$ -order harmonics will be seriously degraded. However, without changing the sampling rate, the proposed FO-NG- $nk \pm m$ RC can be used to improve the frequency adaptive performance. What's more, FO-NG- $nk \pm m$ RC provides a unified framework for integer/fractional-order $nk \pm m$ RCs. Experimental results of FO-NG- $nk \pm m$ RC controlled three-phase PWM inverter system show the effectiveness and advantages of the proposed FO-NG- $nk \pm m$ RC scheme.

INDEX TERMS Error convergence rate, fractional order, $nk \pm m$ -order harmonic, repetitive control, pulse width modulation (PWM) converter.

I. INTRODUCTION

In various industrial applications of PWM converters, e.g. programmable alternating current (AC) power supply [1], uninterruptible power supply (UPS) [2], [3], the harmonic control is an important research problem. Repetitive control (RC) [4], based on internal model principle [5], is an effective control scheme for power converters to track/eliminate periodic reference signal/harmonic disturbance. Compared with conventional RC (CRC), $nk \pm m$ -order harmonic RC ($nk \pm m$ RC) proposed in [6] is more effective for dominating $nk \pm m$ -order harmonics' applications with less data memory and

The associate editor coordinating the review of this manuscript and approving it for publication was Sze Sing Lee .

much faster error convergence rate, such as $4k \pm 1$ RC for single-phase power electronics systems [7] and $6k \pm 1$ RC for three-phase power electronics systems [8]. However, the $nk \pm m$ RC proposed in [6] is a nonstandard RC structure, called 1st-generation $nk \pm m$ RC in this paper. It is not convenient and easy to design $nk \pm m$ RC controller using many existing design approaches and skills of CRC controller. Therefore, in this paper, a new generation of $nk \pm m$ RC (NG- $nk \pm m$ RC) is firstly proposed with standard RC structure.

In many PWM converter applications, the working frequency is not always constant, for example, the grid frequency is practically not a constant but within a certain range (e.g. 59 Hz-61 Hz) [9]. Under such condition, the value of N or N/n in the delay element z^{-N} of digital CRC or $z^{-N/n}$ of

digital $nk \pm m$ RC will not be an integer, where $N = f_s/f_o$, f_s being the sampling frequency and f_o being the fundamental frequency. Thus, the fractional delay (FD) problem in the digital RC will inevitably cause serious degradation of control performance, such as worsen output voltage/current waveform quality and rising total harmonic distortion (THD). Therefore, RC-controlled PWM converters not only need good control performance in the case of integer delay under constant working frequency, but also in the case of FD under frequency variation.

Fractional-order repetitive control (FORC) [10]–[17] and higher-order repetitive control (HORC) [18], [19] can be used to solve the frequency variation problem. However, HORC is usually used in slight frequency variation scenarios, and FORC can not only deal with slight frequency variations, but also be suitable for a wide range of frequency variations. Therefore, compared with HORC, the FO scheme is more suitable for various situations, especially for a wide range of frequency variations.

A FD algorithm based on the finite impulse response (FIR) filter can be used to solve the FD problem [10]–[17], which makes FORC controller be adaptive to the frequency variation. FORC can be widely used in many situations even working frequencies not being constant, such as programmable AC power supply [10], active power filter (APF) [11], [12], off-grid power converter [13], [14], grid-connected power converter [15], [16]. However, FO-CRC still occupies a large amount of data memory cells and has slow dynamic response. Compared with FO-CRC, the conventional FO- $nk \pm m$ RC [17] can save the memory space and quicken the dynamic response. But, it is based on the 1st-generation $nk \pm m$ RC and still has the drawback of 1st-generation $nk \pm m$ RC, such as nonstandard RC structure. Moreover, for the Lagrange interpolation polynomial FIR filter used in [17], all $(M + 1)$ coefficients of the M -order FIR filter need to be updated in real-time to approximate different FDs, which will increase the real-time computational burden of the control system.

Therefore, in this paper, a new generation of $nk \pm m$ RC-based FO- $nk \pm m$ RC (FO-NG- $nk \pm m$ RC), using Lagrange interpolation FD filter based on Taylor Series expansion with Farrow structure to accurately approximate the FD, is proposed. Compared with conventional FO-CRC, FO-NG- $nk \pm m$ RC has faster error convergence rate, compatible with non-integer value of N or N/n . What's more, its excellent frequency robustness and good dynamic response greatly expand its usable range to more practical applications.

To emphasize the originality and contribution of our approach, the main contributions of the presented research work are as follows.

1) This paper proposed a new structure of $nk \pm m$ RC, i.e. NG- $nk \pm m$ RC. Compared with conventional $nk \pm m$ RC, it has more streamlined controller structure and more convenient RC design method. While achieving the same controller performance as the conventional $nk \pm m$ RC, NG- $nk \pm m$ RC has more advantages. Moreover, a complete set of RC design methods is given, which is helpful for RC design.

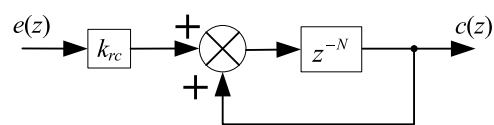


FIGURE 1. Standard RC structure or CRC.

2) This paper proposed a Taylor Series expansion-based FD filter with Farrow structure. In this paper, different FD filter coefficient updating methods are analyzed. The reason why the proposed Taylor Series expansion-based FD filter is superior to the conventional Lagrange interpolation FIR FD filter is explained from the perspective of the controller's computational burden for the first time. The inner relationship between Taylor Series expansion method and Farrow structure FD filter is explained, detailed mathematical derivation is provided, and a complete set of FD filter design methods is formed.

3) The fractional-order scheme is combined with the new structure $nk \pm m$ RC (NG- $nk \pm m$ RC) for the first time, FO-NG- $nk \pm m$ RC system is described, and the stability criterion and stability proof of FO-NG- $nk \pm m$ RC system are given.

The remainder of this paper is organized as follows: In Section II, NG- $nk \pm m$ RC is proposed, whose structural novelty with standard RC structure is introduced and explained. Section III introduces the approximation method of FD used in RC controller. Lagrange interpolation FD filter based on Taylor Series expansion is used to accurately approximate the FD, and Farrow structure makes it efficient. The comparisons between Taylor Series expansion-based FD filter and conventional Lagrange interpolation method FIR FD filter are given. In Section IV, digital FO-NG- $nk \pm m$ RC is proposed, and the general design steps for digital FO-NG- $nk \pm m$ RC are given. In Section V, an application case for RC-controlled three-phase PWM inverter, with four RC controllers, i.e. CRC, $6k \pm 1$ RC, FO-NG-CRC, FO-NG- $6k \pm 1$ RC, is introduced, and their performances are experimentally compared in the case of integer-order delay and fractional-order delay. Experimental results show the effectiveness and advantages of the proposed FO-NG- $nk \pm m$ RC control scheme. Section VI concludes the paper.

II. NEW GENERATION OF $nk \pm m$ RC

A. STANDARD RC STRUCTURE & 1ST-GENERATION OF $nk \pm m$ RC

Standard RC structure, i.e. conventional RC (CRC) structure, is shown in Fig. 1, whose transfer function is as follows:

$$G_{rc}(z) = k_{rc} \cdot \frac{z^{-N}}{1 - z^{-N}} \quad (1)$$

Standard RC structure has many advantages. For example, it enables RC to easily realize the phase lead compensation filter with noncausal component.

However, the 1st-generation of $nk \pm m$ RC proposed in [6] shown in Fig. 2 does not conform to the standard RC

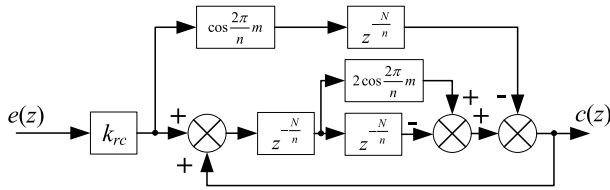


FIGURE 2. 1st-generation of digital $nk \pm m$ RC.

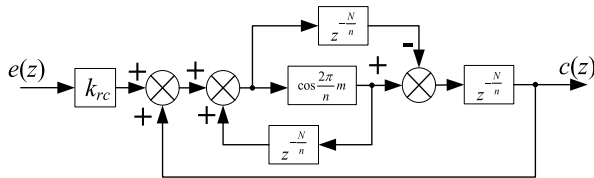


FIGURE 3. New generation of $nk \pm m$ RC.

structure, whose transfer function is shown as follows:

$$G_{nk \pm m}(z) = k_{rc} \cdot \frac{\cos(2\pi m/n) \cdot z^{-N/n} - z^{-2N/n}}{z^{-2N/n} - 2\cos(2\pi m/n) \cdot z^{-N/n} + 1} \quad (2)$$

where $n, m \in \mathbb{N}$ with $n > m \geq 0$.

The structure of 1st-generation of $nk \pm m$ RC is complex, including a negative feedforward gain module and a positive feedforward gain one. Due to its non-standard structure, the complexity of realizing the lead compensator is also increased.

Therefore, it is necessary to present a new generation of $nk \pm m$ RC with standard and simplified RC structure.

B. NEW GENERATION OF $nk \pm m$ RC

The new generation of $nk \pm m$ RC (NG- $nk \pm m$ RC) is shown in Fig. 3, whose transfer function is exact the same with that of the 1st-generation of $nk \pm m$ RC in (2). So, both $nk \pm m$ RCs can achieve complete tracking/elimination of $nk \pm m$ -order harmonics.

As shown in Fig. 3, three delay elements and a positive feedforward gain module form a whole, analogous to z^{-N} in Fig. 1, placed in the forward path. Therefore, NG- $nk \pm m$ RC conforms to the standard RC structure.

Compared with 1st-generation $nk \pm m$ RC, the structure of NG- $nk \pm m$ RC is more streamlined and more convenient to be designed and used, which is only composed of three identical time delay elements, a RC gain module and a positive feedforward gain module.

Similar with the 1st-generation $nk \pm m$ RC, by assigning specific values to n and m in Fig 3 and (2), various NG- $nk \pm m$ RCs can be obtained. For example, letting $n = 1$ and $m = 0$, NG-CRC (equivalent to CRC) can be achieved; letting $n = 4$ and $m = 1$, NG-4 $k \pm 1$ RC (equivalent to odd-harmonic RC, i.e. OHRC [7], [20]) can be achieved; letting $n = 6$ and $m = 1$, NG-6 $k \pm 1$ RC can be achieved.

From Fig. 3, the longest delay length in the forward channel is $2N/n$ times of the sampling period ($< N$, when $n > 2$), and the total memory cells are $(3N/n)$ ($< N$, when $n > 3$).

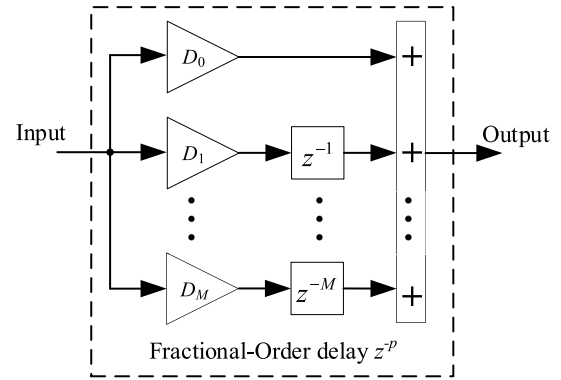


FIGURE 4. Conventional Lagrange interpolation method FIR FD filter.

Obviously, compared with CRC, the proposed NG- $nk \pm m$ RC occupies less memory space and can offer better transient response.

III. TAYLOR SERIES EXPANSION-BASED FD FILTER WITH FARROW STRUCTURE

A. CONVENTIONAL LAGRANGE INTERPOLATION FD FILTER

The conventional Lagrange interpolation FIR FD filter used in [17] can be expressed as:

$$z^{-p} \approx \sum_{l=0}^M D_l z^{-l} \quad (3)$$

and

$$D_l = \prod_{\substack{i=0 \\ i \neq l}}^M \frac{p-i}{l-i}, \quad l = 0, 1, 2, \dots, M \quad (4)$$

where M is the order of the FD filter and D_l is the Lagrange interpolation polynomial coefficient.

Fig. 4 shows the structure of conventional Lagrange interpolation method FIR FD filter. The conventional Lagrange interpolation method FD filter requires different number of multiplications and summations (depending on the order M) to update its output. When the desired approximate FD changes, the whole FD filter needs to be redesigned online, all $M + 1$ coefficients needs to be updated using (4), and the fractional number p needs to participate in the calculation, which greatly increase the design difficulty and complexity of the filter, and even affects the stability of the system.

In order to simplify the structure of FD filter and reduce the computational burden of controller, it is necessary to adopt an efficient FD filter, i.e. Taylor Series expansion-based FD filter with Farrow structure.

B. TAYLOR SERIES EXPANSION-BASED FD FILTER AND ITS DESIGN METHOD

In the implementation of conventional 1st-generation of $nk \pm m$ RC [6], the working fundamental frequency is assured to be constant and the value of N/n in the time delay $z^{-N/n}$ is

also taken as an integer to make the RC controlled system work well. If the working frequency f_0 is varied from the constant value and thus the actual value of $f_s/f_0/n$ is non-integer, a serious degradation of the control performance will be brought out from a constant integer value of N/n . Therefore, it is necessary to apply a FD z^{-p} to the time delay $z^{-N/n}$, i.e. $z^{-N/n} = z^{-\text{round}(N/n)} \cdot z^{-p}$.

According to the design method of FD filter [21], the FD z^{-p} can be well approximated by a FD filter with a linear combination of integer order delays.

Using Taylor Series expansion, the FD $a_n(p) = z^{-p} = e^{-j\omega p}$, where $0 \leq p < 1$, can be expressed as a polynomial of p as follows [22]–[24]:

$$\begin{aligned}
 e^{-j\omega p} &= \sum_{k=0}^{\infty} \frac{(-p)^k}{k!} (j\omega)^k \\
 &= \sum_{k=0}^M \frac{(-1)^k}{k!} (j\omega)^k p^k + p^{M+1} \\
 &\quad \times \left[\sum_{k=M+1}^{\infty} \frac{(-p)^k}{k!} (j\omega)^k p^{k-(M+1)} \right] \\
 &= \sum_{k=0}^M \frac{(-1)^k}{k!} (j\omega)^k p^k + O(p^{M+1}) \quad (5)
 \end{aligned}$$

where M is the polynomial order, the term $O(p^{M+1})$ approaches zero when M is large. So, we can get:

$$a_n(p) = e^{-j\omega p} = \sum_{k=0}^M a_{nk} p^k \approx \sum_{k=0}^M \frac{(-j\omega)^k}{k!} (p)^k \quad (6)$$

In [21] and [25], the FD filter has the following standard form:

$$G_p(z) = \sum_{n=0}^S a_n(p) z^{-n} \quad (7)$$

where S is the order of the FD filter, $a_n(p)$ is a polynomial function of p .

Substituting (6) into (7), FD filter $G_p(z)$ with Farrow structure [25] can be obtained:

$$G_p(z) = \sum_{k=0}^M \sum_{n=0}^S a_{nk} z^{-n} p^k = \sum_{k=0}^M L_k(z) p^k \quad (8)$$

where $L_k(z)$ ($k = 0, 1 \dots M$) is the k^{th} sub-filter in $G_p(z)$, which can be implemented by IIR or FIR filter [21], [26]–[28], and is included into $G_p(z)$ as shown in Fig. 5 [23], [29].

From (5)–(8), the inner relationship between Taylor Series expansion method and Farrow structure FD filter is explained.

The sub-filter $L_k(z)$ ($k = 0, 1 \dots M$) with Farrow structure can be expressed using an S -order polynomial with constant coefficients, where $S \geq M$. To calculate these sub-filters, S is usually selected to be $S = M$ for convenience. The sub-filter

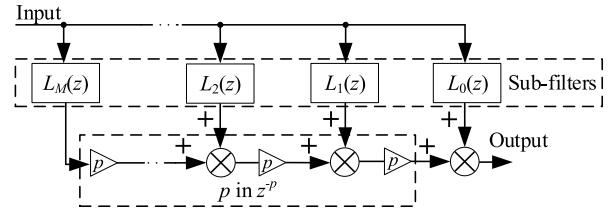


FIGURE 5. Taylor Series expansion-based FD filter $G_p(z)$ with farrow structure.

based on Lagrange interpolation can be calculated as follows [30], [31]:

$$U = \begin{bmatrix} 0^0 & 0^1 & 0^2 & \dots & 0^S \\ 1^0 & 1^1 & 1^2 & \dots & 1^S \\ 2^0 & 2^1 & 2^2 & \dots & 2^S \\ \vdots & \vdots & \vdots & \ddots & \vdots \\ M^0 & M^1 & M^2 & \dots & M^S \end{bmatrix} \quad (9)$$

$$z_{sub} = [1 \quad z^{-1} \quad z^{-2} \quad \dots \quad z^{-M}]^T \quad (10)$$

$$f_{sub} = U^{-1} z_{sub} = [L_0(z) \quad L_1(z) \quad L_2(z) \quad \dots \quad L_M(z)]^T \quad (11)$$

where f_{sub} is the sub-filter matrix, z_{sub} is the delay operator matrix, U is a Vandermonde matrix.

For example, a first-order Farrow structure FD filter can be expressed as:

$$\begin{aligned}
 G_p(z) &= \sum_{k=0}^1 L_k(z) p^k = L_0(z) + L_1(z) p \\
 &= 1 + (z^{-1} - 1) p \quad (12)
 \end{aligned}$$

and a second-order Farrow structure FD filter as:

$$\begin{aligned}
 G_p(z) &= \sum_{k=0}^2 L_k(z) p^k = L_0(z) + L_1(z) p + L_2(z) p^2 \\
 &= 1 + (-1.5 + 2z^{-1} - 0.5z^{-2}) p + (0.5 - z^{-1} + 0.5z^{-2}) p^2 \quad (13)
 \end{aligned}$$

Fig. 6 shows the magnitude response of a first- and second-order Taylor Series expansion-based FD filter $G_p(z)$ using Lagrange interpolation. As can be seen from Fig. 6 that the filter is capable of FD estimation in the low frequency band up to nearly 50% (1500 Hz/3000 Hz, shown in Fig. 6(a)) and 63.5% (1904 Hz/3000 Hz, shown in Fig. 6(b)) of the Nyquist frequency, i.e. 3000 Hz if the sampling frequency being 6000 Hz, for first and second order, respectively. That is to say, the FD can be effectively approximated using the Taylor Series expansion-based FD filter with Farrow structure. It is recommended to choose a second-order filter since it is enough to compromise the complexity and the approximate accuracy.

In contrast, when two FD filters have the same order, using Taylor Series expansion-based FD filter with Farrow structure shown in Fig. 5, only the value of parameter p needs to be adjusted with different frequency conditions and

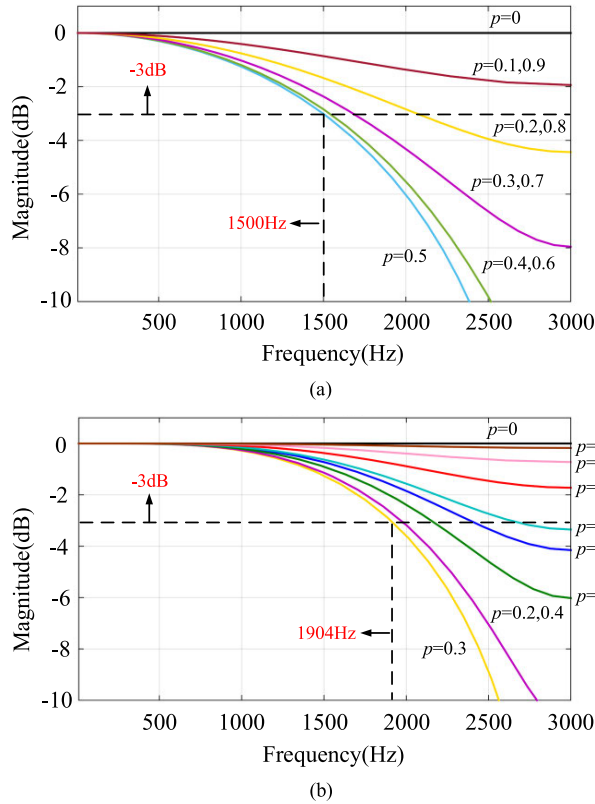


FIGURE 6. The magnitude response of Taylor series expansion-based FD filter $G_p(z)$: (a) First-order FD filter; (b) Second-order FD filter.

thus different FDs. Each sub-filter $L_k(z)$ can be designed offline in advance and do not need to be changed nor any other mathematical calculations, thus greatly reducing the computational burden of the controller.

IV. FO-NG- $nk \pm m$ RC

A. DIGITAL FO-NG- $nk \pm m$ RC

The digital FO-NG- $nk \pm m$ RC can be obtained with the Farrow structure FD filter $G_p(z)$ shown in Fig. 5 embedded in the digital NG- $nk \pm m$ RC shown in Fig. 3. With the low-pass filter $Q(z)$ and phase lead compensation filter $G_f(z)$, the improved digital FO-NG- $nk \pm m$ RC can be achieved and shown in Fig. 7, whose transfer function can be derived as follows:

$$G_{FO-NG-nk \pm m}(z) = k_{rc} \cdot \frac{G_y(z)}{G_x(z)} \cdot G_f(z) \quad (14)$$

where

$$G_y(z) = \cos(2\pi m/n) \cdot z^{-[N/n]} \cdot G_p(z) \cdot Q(z) - z^{-[2N/n]} \cdot G_p^2(z) \cdot Q^2(z) \quad (15)$$

$$G_x(z) = z^{-[2N/n]} \cdot G_p^2(z) \cdot Q^2(z) + 1 - 2 \cos(2\pi m/n) \cdot z^{-[N/n]} \cdot G_p(z) \cdot Q(z) \quad (16)$$

and $[N/n]$ means N/n is rounded down to the nearest integer, e.g. $[5.8] = [5.2] = 5$.

From (14), the transfer function of the improved FO-NG-CRC can be obtained as follows:

$$G_{FO-NG-CRC}(z) = k_{rc} \cdot \frac{z^{-[N]} \cdot G_p(z) \cdot Q(z)}{1 - z^{-[N]} \cdot G_p(z) \cdot Q(z)} \cdot G_f(z) \quad (17)$$

The transfer function of the improved FO-NG- $6k \pm 1$ RC can be obtained as follows:

$$G_{FO-NG-6k \pm 1}(z) = k_{rc} \cdot G_f(z) \cdot \frac{(1/2) z^{-[N/6]} \cdot G_p(z) \cdot Q(z) - z^{-[N/3]} \cdot G_p^2(z) \cdot Q^2(z)}{z^{-[N/3]} \cdot G_p^2(z) \cdot Q^2(z) - z^{-[N/6]} \cdot G_p(z) \cdot Q(z) + 1} \quad (18)$$

It should be pointed out that the NG- $nk \pm m$ RC proposed in this paper is a special case of FO-NG- $nk \pm m$ RC when $p = 0$ ($G_p(z) = 1$).

B. PLUG-IN DIGITAL FO-NG- $nk \pm m$ RC SYSTEM

The FO-NG- $nk \pm m$ RC proposed in this paper is usually plugged into the closed-loop control system as shown in Fig. 8.

Fig. 8 shows a typical closed-loop control system with a plug-in FO-NG- $nk \pm m$ RC controller, where $G_{FO-NG-nk \pm m}(z)$ is a complete improved digital FO-NG- $nk \pm m$ RC controller shown in Fig. 7; $G_p(z)$ is the plant; $G_c(z)$ is the conventional feedback controller; $y_{ref}(z)$ is the reference input; $y(z)$ is the output; $e(z) = y_{ref}(z) - y(z)$ is the tracking error; $c(z)$ is the output of $G_{FO-NG-nk \pm m}(z)$; $u(z)$ is the output of $G_c(z)$ and $d(z)$ is the disturbance.

The actual output of the digital FO-NG- $nk \pm m$ RC system shown in Fig. 8 can be derived into:

$$y(z) = G(z) y_{ref}(z) + G_d(z) d(z) = \frac{[1 + G_{FO-NG-nk \pm m}(z)] \cdot H(z)}{1 + G_{FO-NG-nk \pm m}(z) \cdot H(z)} y_{ref}(z) + \frac{[1 + G_c G_p]^{-1}}{1 + G_{FO-NG-nk \pm m}(z) \cdot H(z)} d(z) \quad (19)$$

where $H(z)$ is the conventional feedback control system without FO-NG- $nk \pm m$ RC controller $G_{FO-NG-nk \pm m}(z)$ plugged into and

$$H(z) = \frac{G_c(z) G_p(z)}{1 + G_c(z) G_p(z)} \quad (20)$$

The error transfer function of the digital FO-NG- $nk \pm m$ RC system can be derived into:

$$T(z) = \frac{e(z)}{y_{ref}(z) - d(z)} = \frac{[1 + G_c G_p]^{-1}}{1 + G_{FO-NG-nk \pm m}(z) \cdot H(z)} \quad (21)$$

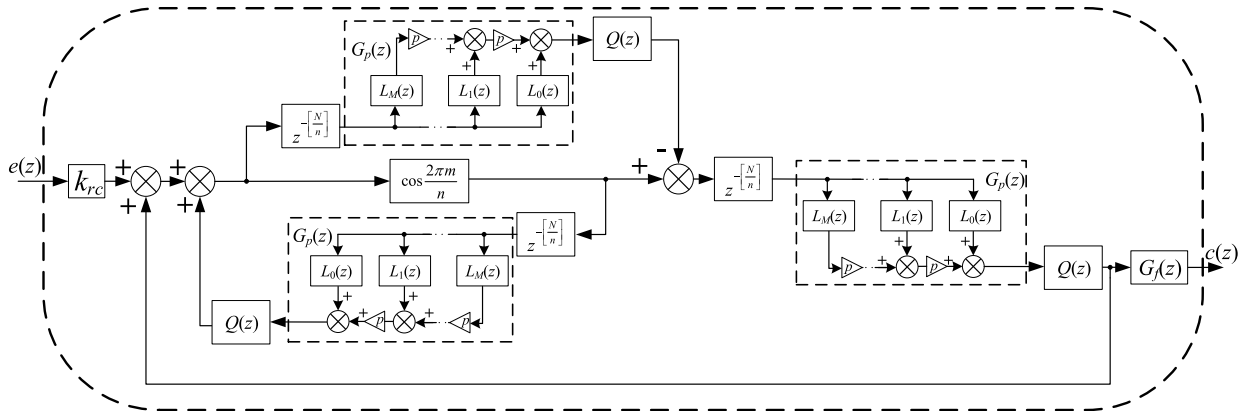


FIGURE 7. Improved digital FO-NG- $nk \pm m$ RC.

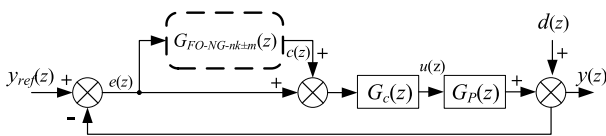


FIGURE 8. Plug-in digital FO-NG- $nk \pm m$ RC system.

From (19)-(21), two stability criteria of the plug-in digital FO-NG- $nk \pm m$ RC system shown in Fig. 8 can be obtained:

- 1) The poles of $H(z)$ are inside the unit circle.
- 2) RC gain k_{rc} ($k_{rc} > 0$) meets the following constraint (See appendix for proof):

$$0 < k_{rc} < \frac{2 \cos(\theta_{fH}(\omega))}{1 + \varepsilon} \quad (22)$$

where $\cos(\theta_{fH}(\omega))$ is the phase angle of $G_f(z)H(z)$ and ε denotes the uncertainty due to model uncertainties of the control plant $G_P(z)$ with $\varepsilon > 0$.

Therefore, two stability criteria for the plug-in digital FO-NG- $nk \pm m$ RC system is obtained.

C. GENERAL DESIGN STEPS FOR DIGITAL FO-NG- $nk \pm m$ RC

Using the general design steps of standard RC structure, it is very easy and convenient to design FO-NG- $nk \pm m$ RC, usually consisting of three parts: Low pass filter $Q(z)$, phase lead compensation filter $G_f(z)$, and the selection of repetitive control gain k_{rc} .

1) LOW PASS FILTER $Q(z)$

In practice, it is usually necessary to add a low-pass filter $Q(z)$ and a phase lead compensator $G_f(z)$ [32]–[35] on the basis of a digital RC controller to improve the stability and robustness of the controller. The design objective of $Q(z)$ is to make $|Q(z)| \rightarrow 1$ at low frequency band and $|Q(z)| \rightarrow 0$ at high frequency band. The low-pass filter $Q(z)$ is usually

selected as a zero-phase low-pass filter:

$$Q(z) = \left[\sum_{i=0}^m \alpha_i z^i + \sum_{i=1}^m \alpha_i z^{-i} \right] / \left[2 \sum_{i=1}^m \alpha_i + \alpha_0 \right] \quad (23)$$

where $\alpha_0 + 2 \sum_{i=1}^m \alpha_i = 1$, and $\alpha_i > 0$.

In practical use, the first-order filter is sufficient, and $Q(z)$ can be selected as:

$$Q(z) = \alpha_1 z + \alpha_0 + \alpha_1 z^{-1} \quad (24)$$

where $2\alpha_1 + \alpha_0 = 1$, $\alpha_0 \geq 0$ and $\alpha_1 \geq 0$.

2) PHASE LEAD COMPENSATION FILTER $G_f(z)$

First, $H(z)$ can be described by

$$H(z) = \frac{B(z)}{A(z)} = \frac{z^{-c} B^+(z) B^-(z)}{A(z)} \quad (25)$$

where c presents known delay steps with $c \in [0, N/n]$, all characteristic roots of $A(z) = 0$ are inside the unit circle, $B^+(z)$ and $B^-(z)$ are the cancelable and un-cancelable parts of $B(z)$, respectively [36]. $B^-(z)$ comprises roots on or outside the unit circle and undesirable roots which are in the unit circle, and $B^+(z)$ comprises of roots of $B(z)$ which are not in $B^-(z)$.

The lead compensation filter $G_f(z)$ can be chosen as [38]:

$$G_f(z) = \frac{z^c A(z) B^-(z^{-1})}{B^+(z) b} \quad (26)$$

where $b \geq \max |B^-(e^{j\omega})|^2$.

Therefore, the product of $G_f(z)$ and $H(z)$ can be written as:

$$G_{fH}(z) = G_f(z) H(z) = \frac{B^-(z^{-1}) B^-(z)}{b} \quad (27)$$

In practical application, there are usually many uncertain factors leading to system delay, and only the $G_f(z)$ determined by actual situation can optimize the performance of RC. Finally, the best $G_f(z)$ needs to be selected through experimental debugging.

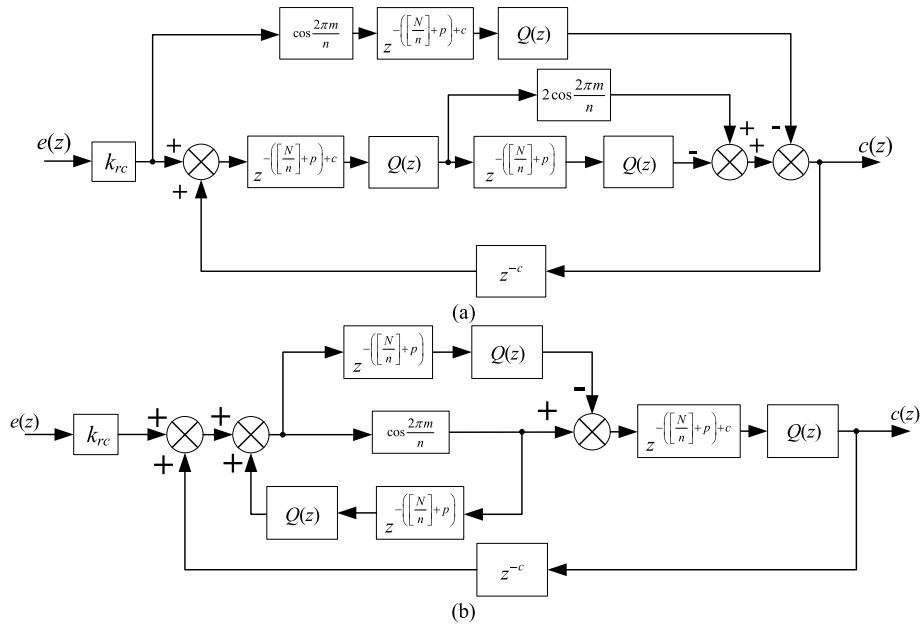


FIGURE 9. The implementation of phase lead compensation filter $G_f(z)$: (a) Conventional FO- $nk \pm m$ RC; (b) FO-NG- $nk \pm m$ RC.

Fig. 9 shows the specific method to implement the phase lead compensation filter $G_f(z)$ of conventional FO- $nk \pm m$ RC (Fig. 9 (a)) and FO-NG- $nk \pm m$ RC (Fig. 9 (b)). The implementation of $G_f(z)$ in FO-NG- $nk \pm m$ RC is easier and more convenient than conventional FO- $nk \pm m$ RC (composed of 1st-generation of $nk \pm m$ RC and Lagrange interpolation method FD filter). As shown in Fig. 9 (a) and (b), compared with conventional FO- $nk \pm m$ RC, FO-NG- $nk \pm m$ RC only needs to realize the lead step z^c after one time delay, which greatly simplifies the implementation complexity of $G_f(z)$ and is hard to make mistakes in actual application.

3) RC GAIN k_{rc}

The selection of repetitive control gain k_{rc} should meet the stability condition of the system, i.e. the stability criteria 2), and finally determined by actual requirements.

V. APPLICATION CASE: FO-NG- $nk \pm m$ RC-CONTROLLED 3-PHASE PWM INVERTER

In order to verify the effectiveness and advantages of the proposed FO-NG- $nk \pm m$ RC, an application case of RC-controlled three-phase PWM inverter is carried out, in which system performances are compared between CRC, $6k \pm 1$ RC, and proposed FO-NG-CRC, FO-NG- $6k \pm 1$ RC in terms of error convergence rate, steady-state performance, load change, and sudden frequency variation. All experiments are based on the new structure of $nk \pm m$ RC (i.e. NG- $nk \pm m$ RC).

A. SYSTEM MODELING AND STATE FEEDBACK CONTROLLER

Fig. 10 shows a three-phase voltage-source PWM inverter system, where E is the DC bus voltage; L and C are

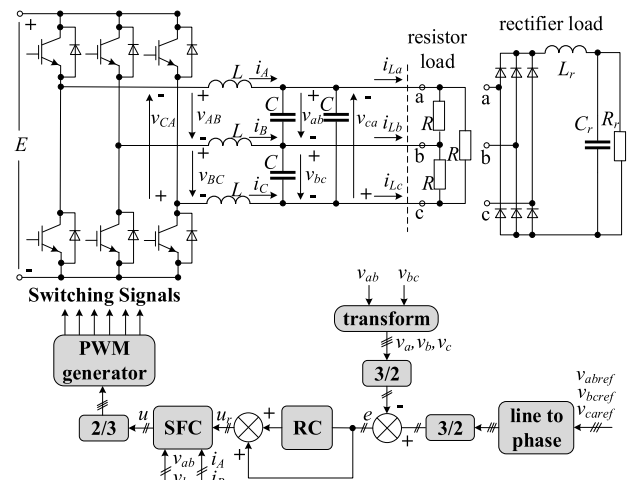


FIGURE 10. RC-controlled three-phase PWM inverter.

inductor–capacitor filter; R is the linear load; and C_r , L_r , and R_r are capacitor, inductor, and resistor in the rectifier load, respectively.

The discrete-time state space equation of the three-phase inverter system in Fig.10 can be written as [37]:

$$\begin{pmatrix} x_1(k+1) \\ x_2(k+1) \end{pmatrix} = \begin{pmatrix} \varphi_{11} & \varphi_{12} \\ \varphi_{21} & \varphi_{22} \end{pmatrix} \begin{pmatrix} x_1(k) \\ x_2(k) \end{pmatrix} + \begin{pmatrix} g_1 \\ g_2 \end{pmatrix} u(k) \quad (28)$$

where $x_1 = v_\alpha$ or v_β , $x_2 = i_\alpha$ or i_β , $u = u_\alpha$ or u_β , and $\varphi_{11} = 1 - T_s/(RC) + T_s^2/(2R^2C^2) - T_s^2/(6LC)$, $\varphi_{12} = T_s/(3C) - T_s^2/(6RC^2)$, $\varphi_{21} = -T_s/L + T_s^2/(2RLC)$, $\varphi_{22} = 1 - T_s^2/(6LC)$, $g_1 = ET_s^2/(6LC)$, $g_2 = ET_s/L$.

The state feedback controller (SFC) [6] has the form as:

$$u = -(k_1x_1 + k_2x_2) + hy_{ref} \quad (29)$$

TABLE 1. System parameters.

Parameters	Value
DC-link voltage E / V	200
Inductor filter L / mH	5
Capacitor filter $C / \mu\text{F}$	100
Rectifier inductor L_r / mH	5
Rectifier capacitor $C_r / \mu\text{F}$	1100
Rectifier load R_r / Ω	60
Reference voltage v_{abref} / V	$120\sin 100\pi t$
Reference voltage v_{bcref} / V	$120\sin(100\pi t - 2\pi/3)$
Reference voltage v_{caref} / V	$120\sin(100\pi t + 2\pi/3)$
Switching and sampling frequency f_s / Hz	6000

where k_1 , k_2 , and h are controller parameters; y_{ref} is the reference sinusoidal voltage. With SFC controller, the state equation of the closed-loop system can be derived into:

$$\begin{pmatrix} x_1(k+1) \\ x_2(k+1) \end{pmatrix} = \begin{pmatrix} \varphi_{11} - g_1k_1 & \varphi_{12} - g_1k_2 \\ \varphi_{21} - g_2k_1 & \varphi_{22} - g_2k_2 \end{pmatrix} \begin{pmatrix} x_1(k) \\ x_2(k) \end{pmatrix} + \begin{pmatrix} g_1h \\ g_2h \end{pmatrix} y_{\text{ref}}(k) \quad (30)$$

The closed-loop system transfer function from y_{ref} to y can be written as:

$$H(z) = \frac{m_1z + m_2}{z^2 + p_1z + p_2} \quad (31)$$

where $p_1 = -[(\varphi_{11} - g_1k_1) + (\varphi_{22} - g_2k_2)]$, $p_2 = -[(\varphi_{12} - g_1k_2)(\varphi_{21} - g_2k_1) - (\varphi_{22} - g_2k_2)(\varphi_{11} - g_1k_1)]$, $m_1 = g_1h$, $m_2 = (\varphi_{12} - g_1k_2)g_2h - (\varphi_{22} - g_2k_2)g_1h$.

The poles of the closed-loop system (31) can be arbitrarily configured by adjusting the SFC gains k_1 and k_2 .

B. EXPERIMENTAL SETUP

An experimental setup of dSPACE 1103-controlled three-phase PWM IGBT inverter system is established. System parameters are shown in TABLE 1.

The following SFC controllers are selected:

$$u = -(1.5606x_1 + 1.775x_2) + 2.322y_{\text{ref}} \quad (32)$$

For a typical three-phase power electronic system, $6k \pm 1$ -order harmonics are dominant. Therefore, the values of n and m are assigned with $n = 6$ and $m = 1$.

To test the control performance under varied frequency and FD condition of RC controllers, reference fundamental frequency is varied from 50 Hz in this paper, and $Q(z) = 0.5z + 0.25 + 0.5z^{-1}$ is selected.

The magnitude response of $Q(z)$ is shown in Fig. 11. It can be seen from Fig. 11 that the cutoff frequency of $Q(z)$ is

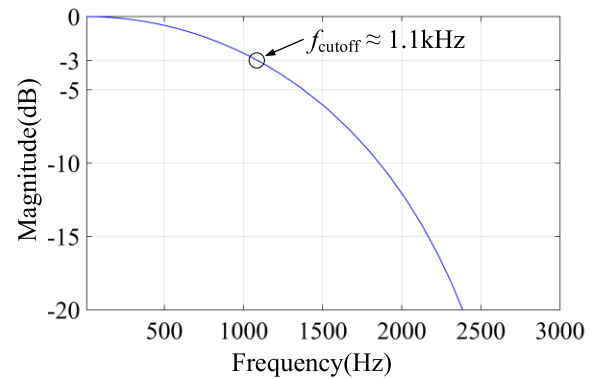


FIGURE 11. Magnitude response of LPF $Q(z)$.

1090 Hz \approx 1100 Hz, which satisfies the design requirement of $Q(z)$. The phase lead compensation filter $G_f(z) = z^8$ and $k_{rc} = 0.3$ are selected by experiments.

C. EXPERIMENTAL RESULTS

Fig.12 (a) and (b) show the steady-state response and error convergence rate of CRC and $6k \pm 1$ RC with reference frequency being 50 Hz under integer delay condition. CRC and $6k \pm 1$ RC are plugged into the SFC controlled three-phase inverter system at $t = 5.375$ s and $t = 5.677$ s, respectively. It should be point out that when the reference frequency is 50 Hz, $N = 120$ for CRC and $N/6 = 20$ for $6k \pm 1$ RC, which is the special case of FO-NG- $nk \pm m$ RC when $p = 0$. Detailed performance comparisons are listed in Table 2.

From Fig. 12 and Table 2, we can get that THDs of output voltage v_{ab} of CRC and $6k \pm 1$ RC are 1.77% and 1.88%, respectively; output voltages' RMS tracking errors of CRC and $6k \pm 1$ RC are 2.30 V and 2.60 V, respectively. It shows that both CRC and $6k \pm 1$ RC have very good steady-state tracking accuracy under integer delay condition. Moreover, from Fig. 12, we can get that the error convergence times of CRC and $6k \pm 1$ RC are 0.73 s and 0.25 s, respectively. The error convergence time of $6k \pm 1$ RC is nearly one third of that of CRC. It shows that $6k \pm 1$ RC has three-time faster error convergence rate than CRC under integer delay condition.

Fig. 13 (a) and (b) show the magnitude response of four controllers with 46 Hz fundamental (reference) frequency and the details of their 5th harmonic frequency, respectively.

As can be seen from Fig. 13 (a), when FD N or N/n occurs, the actual frequency of RC deviates from the ideal frequency. The deviation will increase along with the increase of frequency, which means that the performance of the controller will be seriously affected. Therefore, it is necessary to adopt FO scheme to solve the FD problem.

The $6k \pm 1$ -order harmonics are the dominant harmonics in the three-phase system. Taking the 5th harmonic frequency (230 Hz) of 46 Hz as an example, Fig. 13 (b) shows the details at 5th harmonic frequency. From Fig. 13 (b), we can see that when the fundamental frequency is 46 Hz, the gain of CRC

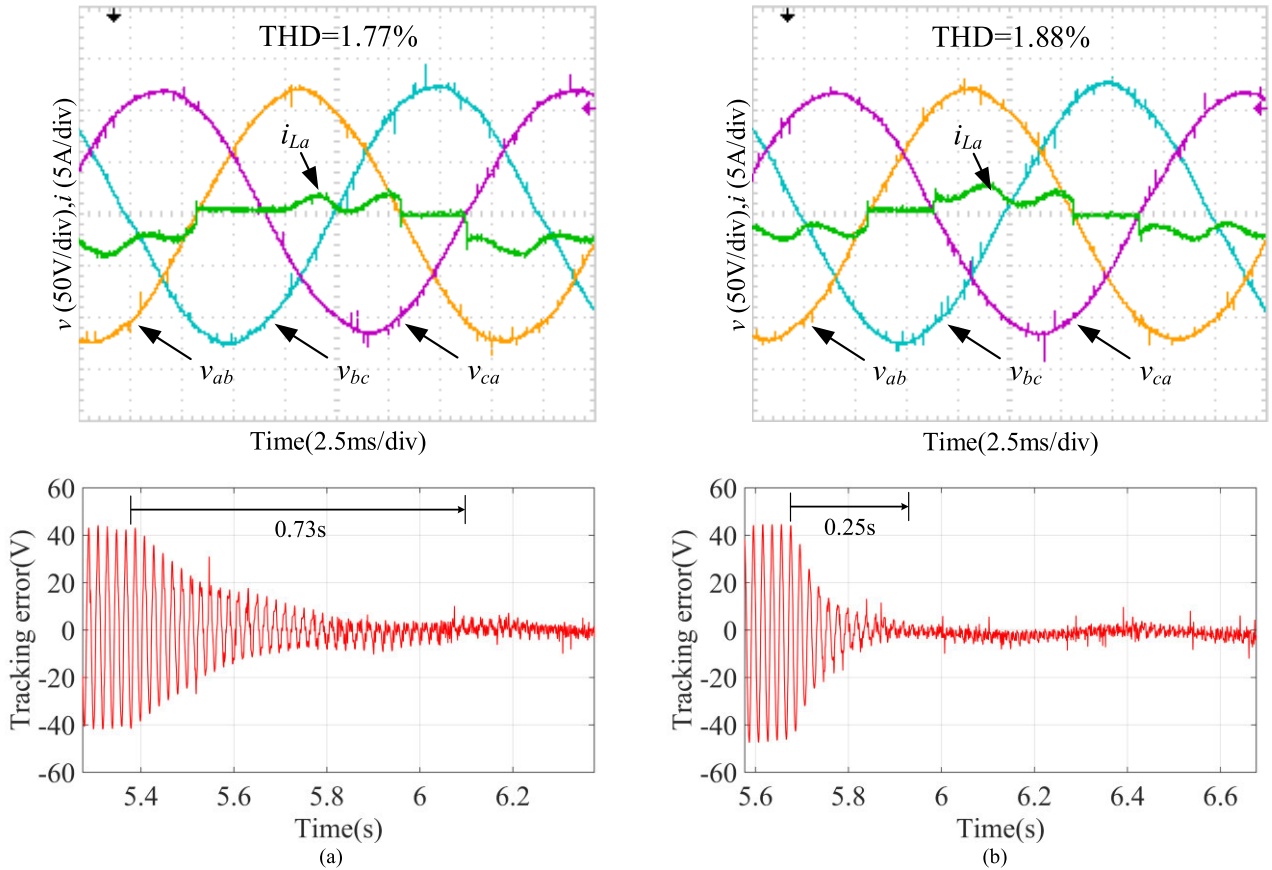


FIGURE 12. Steady-state response and error convergence rate comparison with different plug-in RCs with 50 Hz reference frequency under rectifier load: (a) CRC ($N = 120, p = 0$); (b) $6k \pm 1$ RC ($N/6 = 20, p = 0$).

TABLE 2. Performance comparisons.

Controller	CRC	FO-NG-CRC	$6k \pm 1$ RC	FO-NG- $6k \pm 1$ RC
Frequency (Hz)	46	50	46	46
N	130	120	130.4	22
p	-	0	0.4	20
RMS Tracking error (V)	7.57	2.30	2.25	2.60
THD (%)	3.19	1.77	1.90	2.60
Convergence time (s)	0.65	0.73	0.65	0.23

and $6k \pm 1$ RC at 5th harmonic frequency are 72.3 dB and 18.5 dB, respectively. It also shows that $6k \pm 1$ RC is more sensitive to FD than CRC, so it is necessary to adopt FO scheme. As shown in Fig. 13 (b), with the FO scheme, FO-NG-CRC and FO-NG- $6k \pm 1$ RC can compensate the gain at 5th harmonic frequency to 119 dB and 129 dB, respectively. Obviously, FO-NG- $nk \pm m$ RC will have a better performance than the non-FO one.

Fig. 14 (a) and (b) show the steady-state response and error convergence rate of CRC and FO-NG-CRC with reference frequency being 46 Hz under non-integer delay condition. Under such condition, $N = f_s/f_o = 130.4$. Thus, $N = 130$ has to be taken for CRC. And $[N] + p = 130 + 0.4 = 130.4$ for FO-NG-CRC, where $[N]$ is an integer, and the fractional part p is approximated by a second-order FD filter with Farrow

structure using (13) shown as follows:

$$\begin{aligned}
 z^{-N} &= z^{-[N]} \cdot z^{-p} = z^{-130} \cdot \sum_{k=0}^2 L_k(z) (0.4)^k \\
 &= z^{-130} \cdot \left[1 + (-1.5 + 2z^{-1} - 0.5z^{-2}) (0.4) \right. \\
 &\quad \left. + (0.5 - z^{-1} + 0.5z^{-2}) (0.4)^2 \right] \quad (33)
 \end{aligned}$$

From Fig. 14 and Table 2, we can get that THDs of output voltage v_{ab} of CRC and FO-NG-CRC are 3.19% and 1.90%, respectively; output voltages' RMS tracking errors of CRC and FO-NG-CRC are 7.57 V and 2.25 V, respectively. It shows that FO-NG-CRC has much better steady-state tracking accuracy than CRC under non-integer delay condition. Moreover, from Fig. 14, we can get that the error

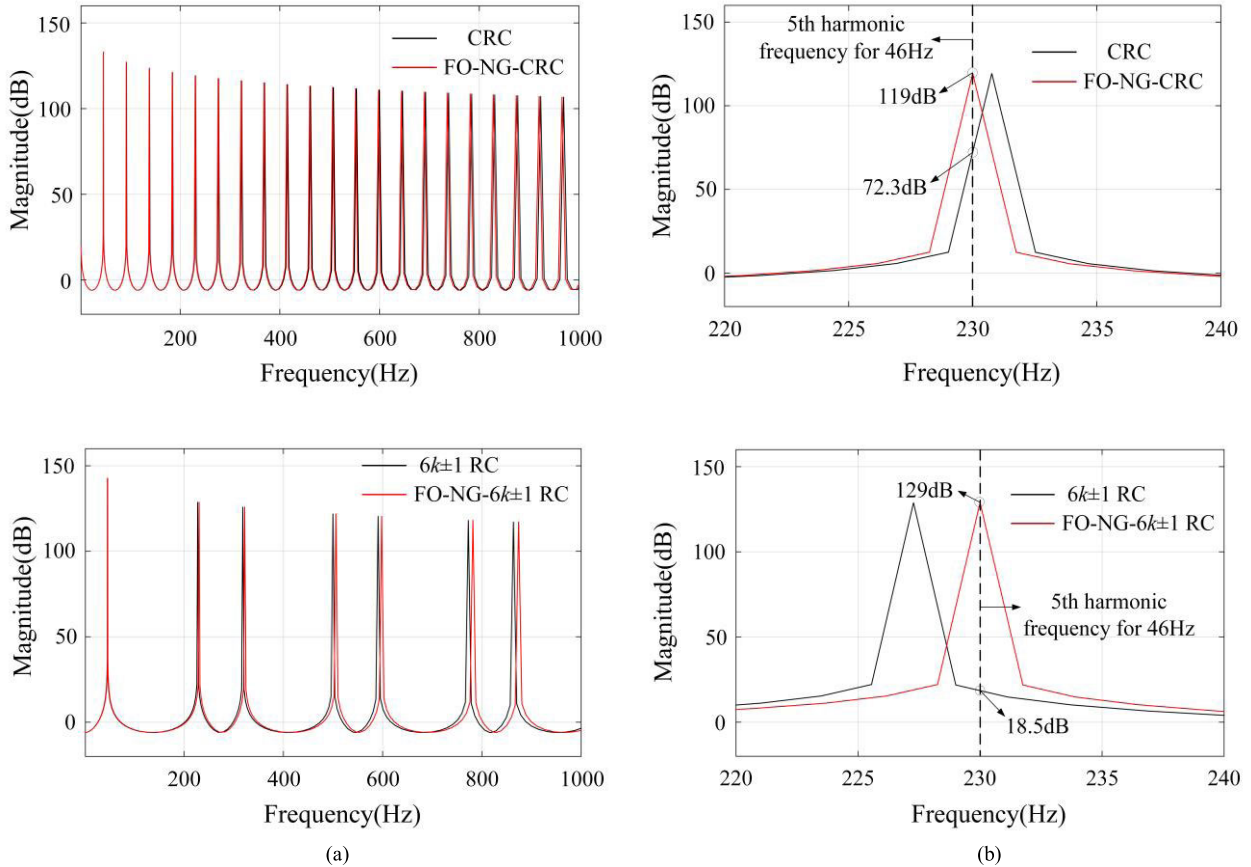


FIGURE 13. Magnitude response of the four controllers and their 5th harmonic frequency with 46 Hz fundamental frequency: (a) CRC ($N = 130$) and FO-NG-CRC ($N = 130.4$); (b) $6k \pm 1$ RC ($N/6 = 22$) and FO-NG- $6k \pm 1$ RC ($N/6 = 21.7$).

convergence times of CRC and FO-NG-CRC are both about 0.65 s. It shows that both CRC and FO-NG-CRC have the same error convergence rate.

Fig. 15 (a) and (b) show the steady-state response and error convergence rate of $6k \pm 1$ RC and the proposed FO-NG- $6k \pm 1$ RC with reference frequency being 46 Hz under non-integer delay condition. Under such condition, $N/6 = f_s/f_o/6 = 21.7$. Thus, $N/6 = 22$, the nearest integer, has to be taken for $6k \pm 1$ RC. And $[N/6] + p = 21 + 0.7 = 21.7$ for FO-NG- $6k \pm 1$ RC, where $[N/6]$ is an integer, the fractional part p is approximated by the second-order FD filter with Farrow structure using (13) shown as follows:

$$\begin{aligned}
 z^{-\frac{N}{6}} &= z^{-\left[\frac{N}{6}\right]} \cdot z^{-p} = z^{-21} \cdot \sum_{k=0}^2 L_k(z) (0.7)^k \\
 &= z^{-21} \cdot \left[1 + (-1.5 + 2z^{-1} - 0.5z^{-2})(0.7) \right. \\
 &\quad \left. + (0.5 - z^{-1} + 0.5z^{-2})(0.7)^2 \right] \quad (34)
 \end{aligned}$$

Similarly, from Fig. 15 and Table 2, we can get that THDs of output voltage v_{ab} of $6k \pm 1$ RC and FO-NG- $6k \pm 1$ RC are 5.28% and 2.37%, respectively; output voltages' RMS tracking errors of $6k \pm 1$ RC and FO-NG- $6k \pm 1$ RC are 9.10 V and 2.80 V, respectively. It shows that FO-NG- $6k \pm 1$ RC has

much better steady-state tracking accuracy than $6k \pm 1$ RC under non-integer delay condition. Moreover, from Fig. 15, we can get that the error convergence times of $6k \pm 1$ RC and FO-NG- $6k \pm 1$ RC are both about 0.23 s. It shows that both $6k \pm 1$ RC and FO-NG- $6k \pm 1$ RC have the same error convergence rate.

It should be noted that the steady-state tracking accuracy of $6k \pm 1$ RC/FO-NG- $6k \pm 1$ RC is slightly lower than that of CRC/FO-NG-CRC. That is because $6k \pm 1$ RC/FO-NG- $6k \pm 1$ RC only tracks/eliminates the dominant $6k \pm 1$ -order harmonics in the three-phase system, but greatly improves the error convergence rate. Therefore, $6k \pm 1$ RC/FO-NG- $6k \pm 1$ RC can achieve a good compromise between tracking accuracy and dynamic response rate.

Fig. 16 and 17 show the transient performance of FO-NG-CRC and FO-NG- $6k \pm 1$ RC with 46 Hz reference frequency under load changes from no load to resistor load and from resistor load to no load, respectively. From Fig. 16, we can see that FO-NG-CRC-controlled output voltages recover from the sudden load changes within twelve cycles, i.e. 0.24 s, while from Fig. 17, FO-NG- $6k \pm 1$ RC-controlled output voltages recover within four cycles, i.e. 0.08 s, which is one third of that of FO-NG-CRC. It shows that FO-NG- $6k \pm 1$ RC has three-time faster voltage recovering rate than

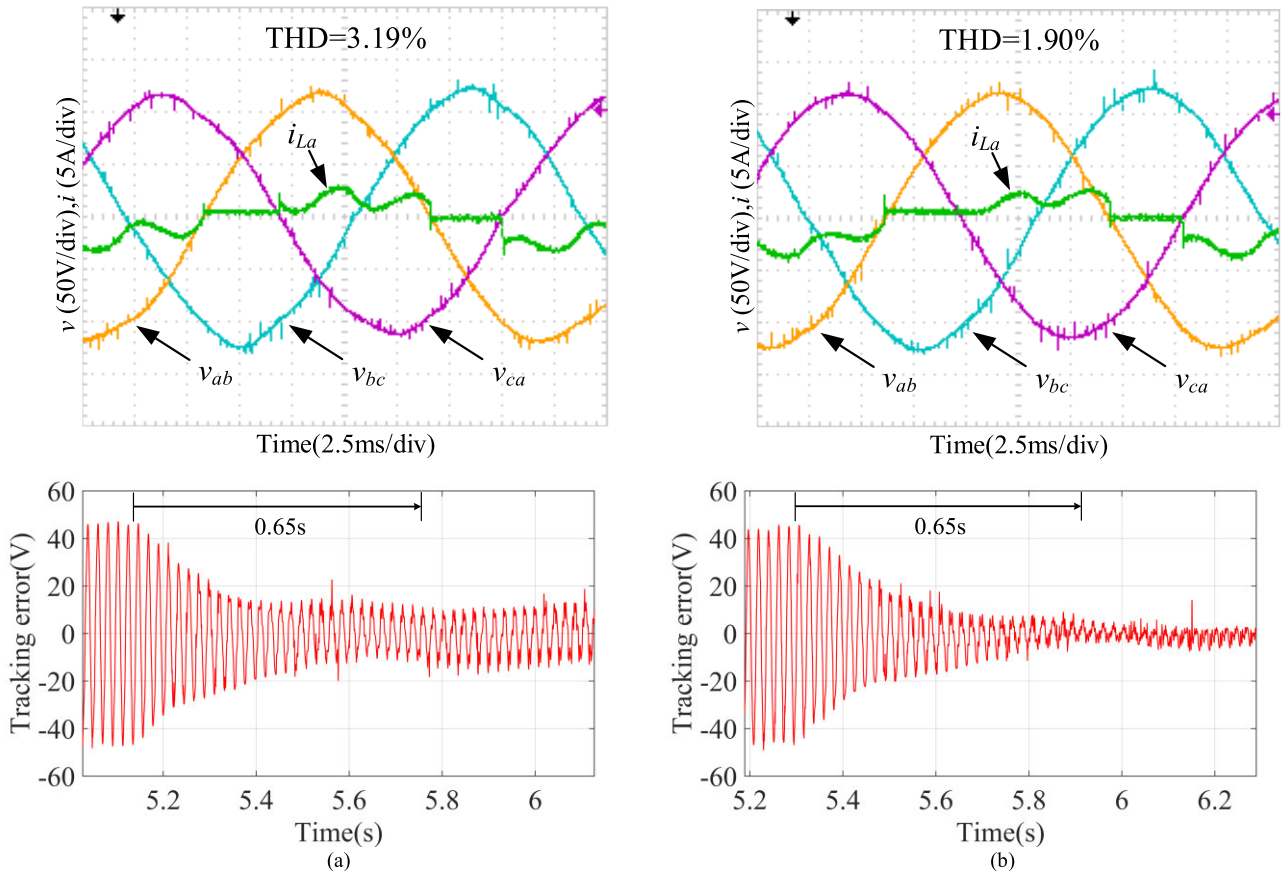


FIGURE 14. Steady-state response and error convergence rate comparison with different plug-in RCs with 46 Hz reference frequency under rectifier load: (a) CRC ($N = 130$); (b) FO-NG-CRC ($N = 130, p = 0.4$).

FO-NG-CRC from the step load change under FD condition. Moreover, both FO-NG-CRC and FO-NG- $6k \pm 1$ RC have a good tracking performance after recovering from the sudden load changes. Therefore, FO-NG-RCs also has excellent adaptability for step load change under fractional order delay.

Fig.18 (a) and (b) show the transient responses of sudden frequency change of $6k \pm 1$ RC and proposed FO-NG- $6k \pm 1$ RC under rectifier load when the reference frequencies are changed from 50 Hz to 60 Hz, i.e. $N/6$ changed from 20 to 16.7, at $t = 10.32$ s and $t = 10.48$ s, respectively. From Fig.18 (a), we can get that the THD of $6k \pm 1$ RC is changed from 1.88% to 2.71% and its RMS error of output voltage v_{ab} changes from 2.60 V to 11.41 V. From Fig.18 (b), we can get that the THD of FO-NG- $6k \pm 1$ RC is changed from 1.88% to 2.23% and its RMS error of output voltage v_{ab} changes from 2.60 V to 2.89 V. Both recovering times of frequency changes of $6k \pm 1$ RC and FO-NG- $6k \pm 1$ RC are 0.2 s. It shows FO-NG- $6k \pm 1$ RC can achieve much higher tracking accuracy when frequency is changed, compared with $6k \pm 1$ RC, and excellent performance of frequency adaptive even the frequency fluctuation being up to 10 Hz. It should be noted that it needs to update FO-NG- $6k \pm 1$ RC's coefficients online to achieve the good tracking performance with FD.

TABLE 3. Computational burden comparisons.

Controller	Fundamental Frequency (Hz)	Turnaround time in DSP (μ s)
CRC	50	18.2
Conventional $6k \pm 1$ RC	50	14.5
NG- $6k \pm 1$ RC	50	14.2
Conventional FO-CRC	46	22.5
FO-NG-CRC	46	20.3
Conventional FO- $6k \pm 1$ RC	46	17.1
FO-NG- $6k \pm 1$ RC	46	16.0

Moreover, the proposed FO-NG- $6k \pm 1$ RC is capable of quickly updating coefficients online.

Table 2 lists the experimental results. The data in Table 2 clearly indicate that FO-NG- $nk \pm m$ RCs-controlled inverter can accurately track the reference signal with fractional delay under rectifier load, and has a fast dynamic response in specific applications.

In order to show the computational burden of various control schemes for the hardware controller more clearly, the turnaround time in DSP of the seven control algorithms mentioned in this paper are compared (Table 3) and the performance indicators are summarized (Table 4).

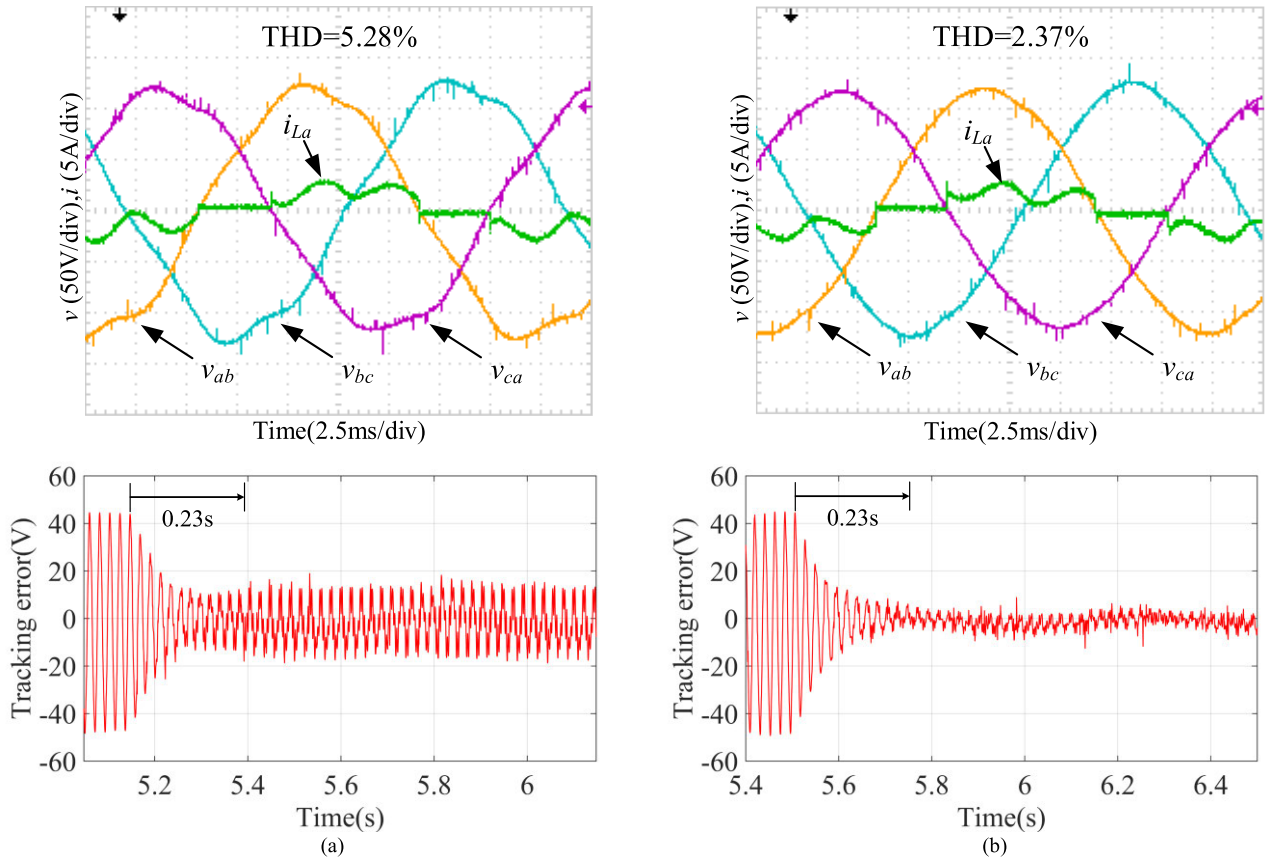


FIGURE 15. Steady-state response and error convergence rate comparison with different plug-in RCs with 46 Hz reference frequency under rectifier load: (a) $6k \pm 1$ RC ($N/6 = 22$); (b) FO-NG- $6k \pm 1$ RC ($N/6 = 21, p = 0.7$).

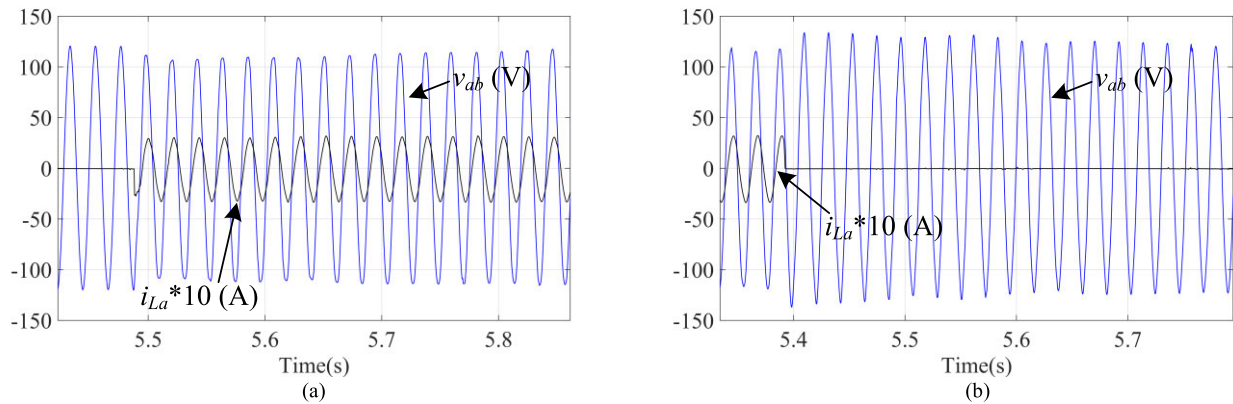


FIGURE 16. Transient performance of FO-NG-CRC with 46 Hz reference frequency under load change: (a) from no load to resistor load; (b) from resistor load to no load.

Table 3 shows the turnaround time of different controllers. As can be seen from Table 3, in the case of integer delay, the value of turnaround time of CRC ($18.2 \mu s$) is larger than that of conventional $6k \pm 1$ RC ($14.5 \mu s$)/NG- $6k \pm 1$ RC ($14.2 \mu s$). That is because the number of delay units used in CRC is larger than that of conventional $6k \pm 1$ RC and NG- $6k \pm 1$ RC. Moreover, NG- $6k \pm 1$ RC, which has a simpler structure and a new phase lead compensation implementation

method, can reduce the memory occupation of the controller to a certain extent.

In the case of fractional delay, the fractional delay filter used in conventional FO- $nk \pm m$ RC needs to update its $M + 1$ coefficients, which increases the computational burden of the controller and occupies more digital resources ($22.5 \mu s$ and $17.1 \mu s$ for conventional FO-CRC and conventional FO- $6k \pm 1$ RC, respectively).

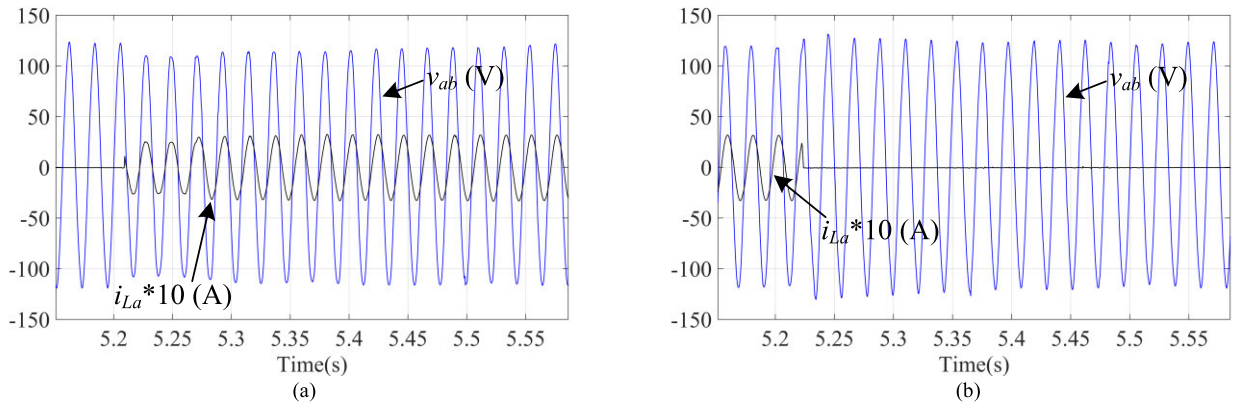


FIGURE 17. Transient performance of FO-NG-6k ± 1 RC with 46 Hz reference frequency under load change: (a) from no load to resistor load; (b) from resistor load to no load.

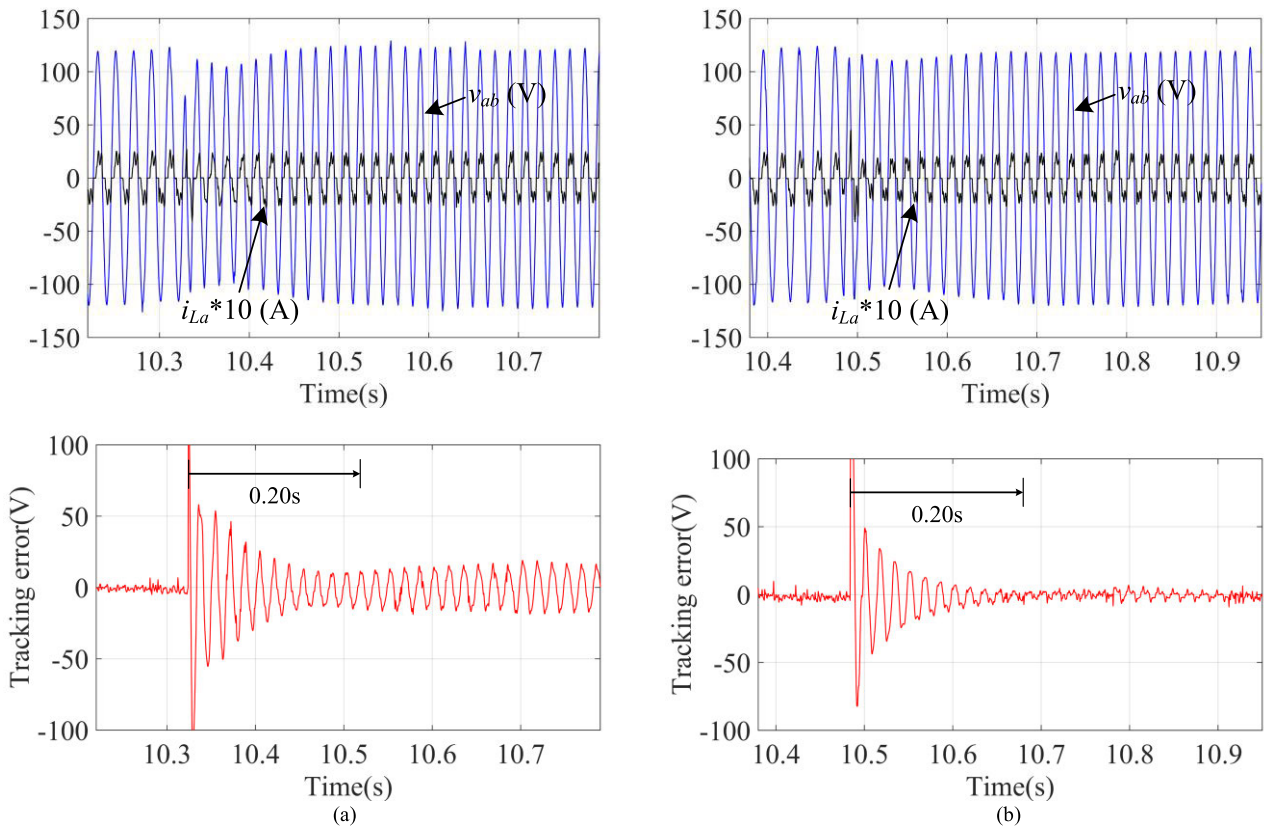


FIGURE 18. Sudden frequency change of different plug-in RCs under rectifier load: 50 Hz → 60 Hz. (a) $6k \pm 1$ RC; (b) FO-NG-6k ± 1 RC.

The control scheme proposed in this paper with Farrow structure fractional delay filter only needs to update one coefficient, i.e. p , which greatly reduces the computational burden of the controller (20.3 μ s and 16.0 μ s for FO-NG-CRC and FO-NG-6k ± 1 RC, respectively), and is a low-cost control scheme. The value of turnaround time of conventional FO-CRC/FO-NG-CRC is larger than that of conventional FO-6k ± 1 RC /FO-NG-6k ± 1 RC is also caused by the large number of delay units.

From Table 3, the NG- $nk \pm m$ RC/FO-NG- $nk \pm m$ RC proposed in this paper occupies fewer digital resources than conventional $nk \pm m$ RC/FO- $nk \pm m$ RC, which is a more efficient structure.

Table 4 summarizes the control schemes mentioned in the paper. In Table 4, more “+” means that the controller occupies more memory space, has higher tracking accuracy, faster error convergence speed or more complex implementation.

TABLE 4. Summary of different control schemes.

Control Scheme	Memory Space	Tracking Accuracy (integer delay)	Tracking Accuracy (fractional delay)	Error Convergence Speed	Complexity
CRC	++	++	+	+	+
$6k \pm 1$ RC	+	+	+	+++	++
NG- $6k \pm 1$ RC	+	+	+	+++	++
FO- $6k \pm 1$ RC	+	+	++	+++	+++
FO-NG- $6k \pm 1$ RC	+	+	++	+++	++

As can be seen from Table 4, the FO-NG- $nk \pm m$ RC proposed in this paper has high tracking accuracy, fast error convergence speed, low memory occupation, and low complexity, which is a cost-effective control scheme and can be fully implemented in microcontrollers.

VI. CONCLUSION

In this paper, a fractional-order new generation of $nk \pm m$ -order harmonic repetitive controller (FO-NG- $nk \pm m$ RC) for PWM converters is proposed. FO-NG- $nk \pm m$ RC is composed of NG- $nk \pm m$ RC and Taylor Series expansion-based FD filter with Farrow structure. NG- $nk \pm m$ RC overcomes the structural defects of conventional $nk \pm m$ RC (1st- generation of $nk \pm m$ RC). The structure of NG- $nk \pm m$ RC is simplified and conforms to the standard RC structure, making it easier and more convenient to be designed and used in practical application. Farrow structure FD filter can approximate FD z^{-p} ($0 \leq p < 1$) using Lagrange interpolation with high accuracy and is easy to be designed and used. The inner relationship between Taylor Series expansion method and Farrow structure FD filter is explained, and detailed mathematical derivation is provided. Different FD approximation algorithms are compared for the first time from the perspective of controller computational burden.

The proposed FO-NG- $nk \pm m$ RC can improve the frequency adaptive ability of the $nk \pm m$ RC controller and increases its usage range. Moreover, FO-NG- $nk \pm m$ RC provides a general RC structure for various integer/fractional-order RCs. The effectiveness and advantages of NG- $nk \pm m$ RC and FO-NG- $nk \pm m$ RC are verified from the experimental results of NG-RCs- and FO-NG-RCs-controlled three-phase PWM inverter.

Furthermore, the FO-NG- $nk \pm m$ RC proposed in this paper can also be applied to grid-connected inverter/rectifier systems and active power filters to solve non-integer delay problems.

APPENDIX

First, $H(z)$ can be expressed by (25), the lead compensation filter $G_f(z)$ can be expressed by (26).

In practice, due to model uncertainties and load variations, it is impossible to obtain the exact transfer function $H(z)$. The practical transfer function of $G_f(z)H(z)$ can be written as:

$$G_{fH}(z) = G_f(z)H(z) = \frac{B^-(z^{-1})B^-(z)}{b}(1 + \Lambda(z))$$

$$\begin{aligned} &= \left| G_{fH}(e^{j\omega}) \right| \angle \theta_{fH}(\omega) \\ &= \left| G_{fH}(e^{j\omega}) \right| e^{j\theta_{fH}(\omega)} \end{aligned} \tag{35}$$

where $\Delta(z)$ denotes the uncertainties assumed to be bounded by $|\Delta(e^{j\omega})| \leq \varepsilon$ with ε being a positive constant, and $\Delta(z)$ is stable.

From (20), since $H(z)$ is assumed to be asymptotically stable, the poles of $(1 + G_c(z)G_p(z))^{-1}$ are then located inside the unit circle. Therefore, from (19), if all the poles of $(1 + G_{FO-NG-nk \pm m}(z)H(z))^{-1}$ are also located inside the unit circle, the overall closed-loop FO-NG- $nk \pm m$ RC system shown in Fig. 8 will be asymptotically stable.

The denominator of $(1 + G_{FO-NG-nk \pm m}(z)H(z))^{-1}$ can be written as:

$$\begin{aligned} &z^{2[N/n]} + (1 - k_{rc} \cdot G_{fH}(z)) \cdot G_p^2(z) \cdot Q^2(z) \\ &+ (k_{rc} \cdot G_{fH}(z) - 2) \cdot G_p(z) \cdot Q(z) \cdot \cos(2\pi m/n) \cdot z^{[N/n]} \end{aligned} \tag{36}$$

which can be factorized as:

$$(z^{[N/n]} - \alpha e^{\beta j}) (z^{[N/n]} - \alpha e^{-\beta j}) \tag{37}$$

where

$$\begin{aligned} \alpha &= \pm (1 - k_{rc} \cdot G_{fH}(z))^{1/2} \cdot G_p(z) \cdot Q(z) \\ \beta &= \pm \frac{(k_{rc} \cdot G_{fH}(z) - 2)}{2(1 - k_{rc} \cdot G_{fH}(z))^{1/2}} \cdot \cos(2\pi m/n) \end{aligned}$$

Therefore, the poles of $(1 + G_{FO-NG-nk \pm m}(z)H(z))^{-1}$ are located inside the unit circle if $|\alpha| < 1$, i.e.:

$$|\alpha| = |Q(z) \cdot G_p(z)| \cdot \left| (1 - k_{rc} \cdot G_{fH}(z))^{1/2} \right| < 1 \tag{38}$$

And then

$$\left| Q(e^{j\omega}) \cdot G_p(e^{j\omega}) \right|^4 \cdot \left| (1 - k_{rc} \cdot \left| G_{fH}(e^{j\omega}) \right| e^{j\theta_{fH}(\omega)}) \right|^2 < 1 \tag{39}$$

$G_p(z)$ is the FD filter, assuming that the bandwidth of the FD filter is larger than the bandwidth of the low-pass filter $Q(z)$ in practical applications, due to $Q(z) \rightarrow 1$, $G_p(z) \rightarrow 1$, then $|Q(e^{j\omega})| \left| \sum_{k=0}^M L_k(z)p^k \right| \rightarrow 1$, thus from (39), if

$$1 - 2k_{rc} \left| G_{fH}(e^{j\omega}) \right| \cos(\theta_{fH}(\omega)) + k_{rc}^2 \left| G_{fH}(e^{j\omega}) \right|^2 < 1 \tag{40}$$

holds, the poles of $(1 + G_{FO-NG-nk \pm m}(z)H(z))^{-1}$ are located inside the unit circle.

Since

$$b \geq \max \left(\left| B^- (e^{j\omega}) \right|^2 \right) = \max \left(B^- (e^{j\omega}) B^- (e^{-j\omega}) \right) > 0 \quad (41)$$

from (35), we have

$$\left| G_{FH} (e^{j\omega}) \right| = \left| \frac{B^- (e^{j\omega}) B^- (e^{-j\omega})}{b} \left(1 + \Delta (e^{j\omega}) \right) \right| \leq 1 + \varepsilon \quad (42)$$

Therefore, from (39) and (42), we can obtain that, if

$$2p\pi - \frac{\pi}{2} < \theta_{FH} (\omega) < 2p\pi + \frac{\pi}{2}, \quad p = 0, 1, 2, \dots$$

then

$$0 < k_{rc} < \frac{2 \cos (\theta_{FH} (\omega))}{1 + \varepsilon} \quad (43)$$

which will enable the closed-loop FO-NG- $nk \pm m$ RC system shown in Fig. 8 to be asymptotically stable; if

$$2p\pi + \frac{\pi}{2} < \theta_{FH} (\omega) < 2p\pi + \frac{3\pi}{2}, \quad p = 0, 1, 2, \dots$$

then

$$\frac{2 \cos (\theta_{FH} (\omega))}{1 + \varepsilon} < k_{rc} < 0 \quad (44)$$

which will enable the closed-loop FO-NG- $nk \pm m$ RC system to be asymptotically stable.

REFERENCES

- [1] Y.-Y. Tzou, R.-S. Ou, S.-L. Jung, and M.-Y. Chang, "High-performance programmable AC power source with low harmonic distortion using DSP-based repetitive control technique," *IEEE Trans. Power Electron.*, vol. 12, no. 4, pp. 715–725, Jul. 1997.
- [2] J. Sik Lim, C. Park, J. Han, and Y. Il Lee, "Robust tracking control of a three-phase DC-AC inverter for UPS applications," *IEEE Trans. Ind. Electron.*, vol. 61, no. 8, pp. 4142–4151, Aug. 2014.
- [3] G. He, M. Chen, W. Yu, N. He, and D. Xu, "Design and analysis of multiloop controllers with DC suppression loop for paralleled UPS inverter system," *IEEE Trans. Ind. Electron.*, vol. 61, no. 12, pp. 6494–6506, Dec. 2014.
- [4] S. Hara, Y. Yamamoto, T. Omata, and M. Nakano, "Repetitive control system: A new type servo system for periodic exogenous signals," *IEEE Trans. Autom. Control*, vol. 33, no. 7, pp. 659–668, Jul. 1988.
- [5] B. A. Francis and W. M. Wonham, "Paper: The internal model principle of control theory," *Automatica*, vol. 12, no. 5, pp. 457–465, Sep. 1976.
- [6] W. Lu, K. Zhou, D. Wang, and M. Cheng, "A generic digital $nk \pm m$ -order harmonic repetitive control scheme for PWM converters," *IEEE Trans. Ind. Electron.*, vol. 61, no. 3, pp. 1516–1527, Mar. 2014.
- [7] K. Zhou, K.-S. Low, D. Wang, F.-L. Luo, B. Zhang, and Y. Wang, "Zero-phase odd-harmonic repetitive controller for a single-phase PWM inverter," *IEEE Trans. Power Electron.*, vol. 21, no. 1, pp. 193–201, Jan. 2006.
- [8] G. Escobar, P. G. Hernandez-Briones, P. R. Martinez, M. Hernandez-Gomez, and R. E. Torres-Olguin, "A repetitive-based controller for the compensation of $6/\pm 1$ harmonic components," *IEEE Trans. Ind. Electron.*, vol. 55, no. 8, pp. 3150–3158, Aug. 2008.
- [9] E. Romero-Cadaval, G. Spagnuolo, L. G. Franquelo, C. A. Ramos-Paja, T. Suntio, and W. M. Xiao, "Grid-connected photovoltaic generation plants: Components and operation," *IEEE Ind. Electron. Mag.*, vol. 7, no. 3, pp. 6–20, Sep. 2013.
- [10] Z. Zou, M. Cheng, Z. Wang, and K. Zhou, "Fractional-order repetitive control of programmable AC power sources," *IET Power Electron.*, vol. 7, no. 2, pp. 431–438, Feb. 2014.
- [11] Z.-X. Zou, K. Zhou, Z. Wang, and M. Cheng, "Frequency-adaptive fractional-order repetitive control of shunt active power filters," *IEEE Trans. Ind. Electron.*, vol. 62, no. 3, pp. 1659–1668, Mar. 2015.
- [12] C. Xie, K. Li, X. Zhao, J. C. Vasquez, and J. M. Guerrero, "Enhanced fractional-order repetitive control for three-phase active power filter," in *Proc. IEEE Appl. Power Electron. Conf. Expo. (APEC)*, Mar. 2017, pp. 3329–3336.
- [13] Y. Wang, D. Wang, B. Zhang, and K. Zhou, "Fractional delay based repetitive control with application to PWM DC/AC converters," in *Proc. IEEE Int. Conf. Control Appl.*, Singapore, 2007, pp. 928–933.
- [14] Q. Zhao and Y. Ye, "Fractional phase lead compensation RC for an inverter: Analysis, design, and verification," *IEEE Trans. Ind. Electron.*, vol. 64, no. 4, pp. 3127–3136, Apr. 2017.
- [15] K. Zhou, Y. Yang, and F. Blaabjerg, "Frequency adaptive repetitive control of grid-tied single-phase PV inverters," in *Proc. Eur. Conf. Cognit. Ergonom.*, 2015, pp. 1689–1693.
- [16] D. Chen, J. Zhang, and Z. Qian, "An improved repetitive control scheme for grid-connected inverter with frequency-adaptive capability," *IEEE Trans. Ind. Electron.*, vol. 60, no. 2, pp. 814–823, Feb. 2013.
- [17] Y. Yang, K. Zhou, H. Wang, F. Blaabjerg, D. Wang, and B. Zhang, "Frequency adaptive selective harmonic control for grid-connected inverters," *IEEE Trans. Power Electron.*, vol. 30, no. 7, pp. 3912–3924, Jul. 2015.
- [18] M. Steinbuch, "Repetitive control for systems with uncertain period-time," *Automatica*, vol. 38, no. 12, pp. 2103–2109, Dec. 2002.
- [19] M. Jamil, A. Waris, S. O. Gilani, B. A. Khawaja, M. N. Khan, and A. Raza, "Design of robust higher-order repetitive controller using phase lead compensator," *IEEE Access*, vol. 8, pp. 30603–30614, 2020, doi: 10.1109/ACCESS.2020.2973168.
- [20] R. Griñó and R. Costa-Castelló, "Digital repetitive plug-in controller for odd-harmonic periodic references and disturbances," *Automatica*, vol. 41, no. 1, pp. 153–157, Jan. 2005.
- [21] T. I. Laakso, V. Valimäki, M. Karjalainen, and U. K. Laine, "Splitting the unit delay [FIR/all pass filters design]," *IEEE Signal Process. Mag.*, vol. 13, no. 1, pp. 30–60, Jan. 1996.
- [22] T. Moller, R. Machiraju, K. Mueller, and R. Yagel, "Evaluation and design of filters using a Taylor series expansion," *IEEE Trans. Vis. Comput. Graphics*, vol. 3, no. 2, pp. 184–199, Apr. 1997.
- [23] A. Eghbali, H. Johansson, and T. Saramäki, "A method for the design of farrow-structure based variable fractional-delay FIR filters," *Signal Process.*, vol. 93, no. 5, pp. 1341–1348, May 2013.
- [24] S.-C. Pei and C.-C. Tseng, "An efficient design of a variable fractional delay filter using a first-order differentiator," *IEEE Signal Process. Lett.*, vol. 10, no. 10, pp. 307–310, Oct. 2003.
- [25] C. W. Farrow, "A continuously variable digital delay element," in *Proc. IEEE Int. Symp. Circuits Syst.*, 1988, pp. 2641–2645.
- [26] M. Makundi and T. I. Laakso, "Efficient symbol synchronization techniques using variable FIR or IIR interpolation filters," in *Proc. Int. Symp. Circuits Syst.*, 2003, pp. 570–573.
- [27] D. Babic, J. Vesma, T. Saramäki, and M. Renfors, "Implementation of the transposed farrow structure," in *Proc. IEEE Int. Symp. Circuits Systems. Process.*, 2002, pp. 5–8.
- [28] C. Tseng, "Design of variable fractional delay FIR filter using differentiator bank," in *Proc. Int. Symp. Circuits Syst.*, 2002, pp. 421–424.
- [29] K. Rajalakshmi, S. Gondi, and A. Kandaswamy, "A fractional delay FIR filter based on Lagrange interpolation of Farrow structure," *Int. J. Electr. Electron. Eng.*, vol. 1, no. 5, pp. 103–107, 2012.
- [30] V. Valimäki, "A new filter implementation strategy for Lagrange interpolation," in *Proc. Int. Symp. Circuits Syst.*, 1995, pp. 361–364.
- [31] R. Nazir, A. Wood, H. Laird, and N. Watson, "An adaptive repetitive controller for three-phase PWM regenerative rectifiers," in *Proc. Int. Conf. Renew. Energy Res. Appl. (ICRERA)*, Nov. 2015, pp. 1126–1131.
- [32] K. Zhou, D. Wang, B. Zhang, Y. Wang, J. A. Ferreira, and S. W. De Haan, "Dual-mode structure digital repetitive control," *Automatica*, vol. 43, no. 3, pp. 546–554, Mar. 2007.
- [33] K. Zhou, D. Wang, B. Zhang, and Y. Wang, "Plug-in Dual-Mode-Structure repetitive controller for CVCF PWM inverters," *IEEE Trans. Ind. Electron.*, vol. 56, no. 3, pp. 784–791, Mar. 2009.
- [34] B. Zhang, D. Wang, K. Zhou, and Y. Wang, "Linear phase lead compensation repetitive control of a CVCF PWM inverter," *IEEE Trans. Ind. Electron.*, vol. 55, no. 4, pp. 1595–1602, Apr. 2008.
- [35] B. Zhang, K. Zhou, Y. Wang, and D. Wang, "Performance improvement of repetitive controlled PWM inverters: A phase-lead compensation solution," *Int. J. Circuit Theory Appl.*, vol. 38, no. 5, pp. 453–469, 2010.

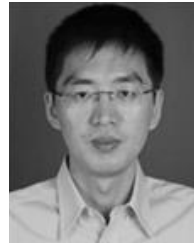
- [36] C. Cosner, G. Anwar, and M. Tomizuka, "Plug in repetitive control for industrial robotic manipulators," in *Proc. IEEE Proceedings. Int. Conf. Robot. Autom.*, 1990, pp. 1970–1975.
- [37] K. Zhou and D. Wang, "Digital repetitive learning controller for three-phase CVCF PWM inverter," *IEEE Trans. Ind. Electron.*, vol. 48, no. 4, pp. 820–830, Aug. 2001.



WEI WANG received the B.S. degree from Jilin Normal University, Jilin, China, in 2018. He is currently pursuing the M.S. degree with the School of Internet of Things (IoT) Engineering, Jiangnan University, Wuxi, China. His research interests include power electronics and its control.



WENZHOU LU (Member, IEEE) received the B.Sc. degree from Jiangsu University, Zhenjiang, China, in 2007, and the Ph.D. degree from Southeast University, Nanjing, China, in 2013. He is currently working with the School of Internet of Things (IoT) Engineering, Jiangnan University, Wuxi, China, as an Associate Professor. From February 2012 to August 2012, he was a Visiting Research Student at Nanyang Technological University, Singapore. He has authored or coauthored more than 30 technical articles and holds patents in his relevant research areas. His teaching and research interests include power electronics and its control, renewable energy generation, and wireless power transfer technology.



KELIANG ZHOU (Senior Member, IEEE) received the B.Sc. degree from the Huazhong University of Science and Technology, Wuhan, China, in 1992, the M.Eng. degree from the Wuhan University of Technology, Wuhan, in 1995, and the Ph.D. degree in electrical engineering from Nanyang Technological University, Singapore, in 2002. He is currently working as a Professor with the School of Automation, Wuhan University of Technology. He has authored or coauthored one monograph, the periodic control of power electronic converters, and more than 100 technical articles. He holds several granted patents in his relevant research areas. His current research interests include power electronics and electric drives, renewable energy generation, control theory and its applications, and microgrid technology.



QIGAO FAN (Member, IEEE) received the B.S. and M.S. degrees in control and instrumentation and the Ph.D. degree in mechatronics engineering from the China University of Mining Technology, Xuzhou, China, in 2008, 2010, and 2013, respectively. In 2013, he joined Jiangnan University, Wuxi, China, as a Lecturer. He is currently an Associate Professor of electrical engineering with the School of Internet of Things (IoT), Jiangnan University. His research interests include indoor localization, robotics, intelligent casting, wireless microelectromechanical system-based technologies, and the IoT sensor technology.

• • •